

DESIGN OF SUPERSONIC COANDA JET NOZZLES*

Paul M. Bevilaqua
 Lockheed Advanced Aeronautics Company
 John D. Lee
 Ohio State University, Columbus, Ohio

ABSTRACT

The thrust vectoring of supersonic Coanda jets was experimentally studied to determine the effect of skewing the initial velocity profile to eliminate expansion and turning shocks. A new nozzle design procedure, based on the method of characteristics, was developed to design an asymmetric convergent-divergent nozzle for skewing the velocity profile. The performances of a simple convergent nozzle, a symmetric C-D nozzle, and an asymmetric C-D nozzle were experimentally compared over a range of pressure ratios from 1.5 to 3.5. Eliminating the expansion shocks with the symmetric C-D nozzle was found to improve the thrust vectoring; skewing the velocity profile to eliminate the turning shocks further improved the vectoring.

NOMENCLATURE

k	Vorticity Factor	∂	Differential Operator
\dot{m}	Mass Flow Rate	Δ	Difference Operator
M	Mach Number	δ	Local Jet Thickness
P	Pressure	r	Ratio of Specific Heats
PR	Pressure Ratio	ρ	Jet Density
R	Radius of Curvature	τ	Temperature
R	Gas Constant	θ	Flow Angle
Re	Reynolds Number	ν	Prandtl-Myer Function
T	Jet Momentum	γ	Ratio of Specific Heats
t	Nozzle Gap	<u>Subscripts</u>	
r, ϕ	Polar Coordinates	∞	Infinity
x, y	Cartesian Coordinates	sep	Separation
V	Jet Velocity	o	Stagnation

INTRODUCTION

A particularly simple and, therefore, attractive means of developing the additional lift required by V/STOL aircraft is to utilize the Coanda effect to deflect the engine exhaust jet, as shown in Figure 1. The Coanda effect is the tendency for a fluid jet to attach itself to an adjacent surface and follow its contour. The jet is pulled onto the surface by the low pressure region which develops as entrainment pumps fluid from the region between the jet and the surface. The jet is then held to the wall by the resulting radial pressure gradient, which balances the jet's inertial resistance to turning.

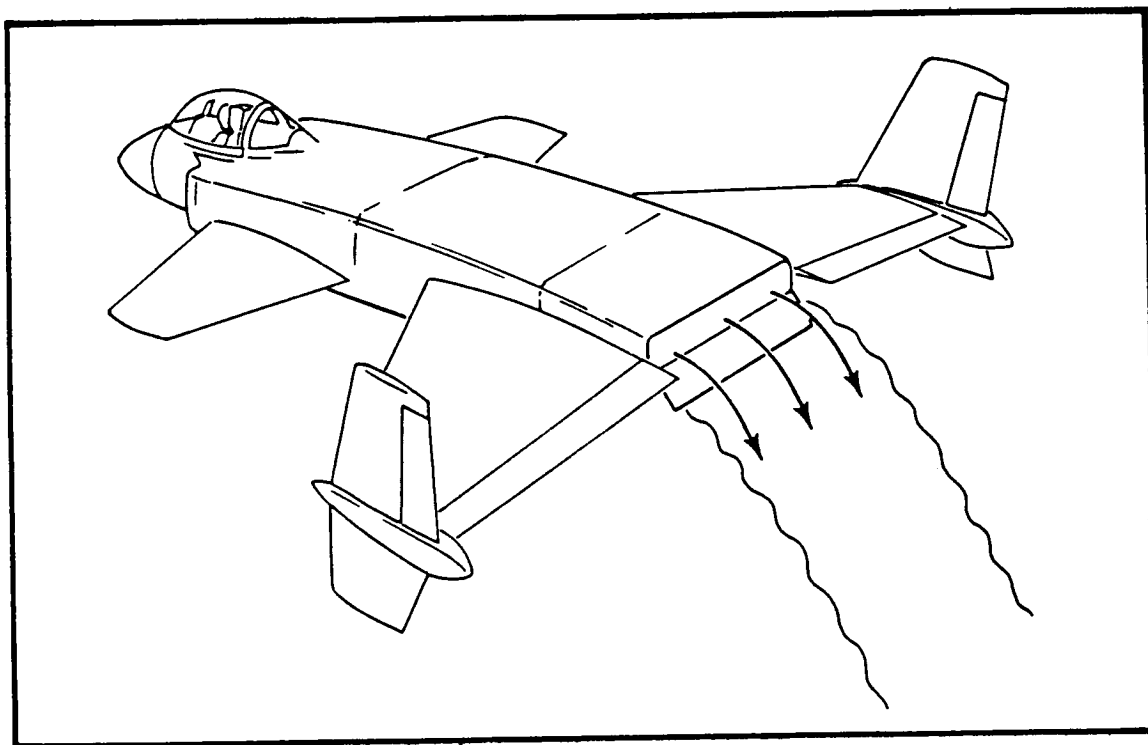


Figure 1. Use of the Coanda Effect for Thrust Vectoring

If the radius of the Coanda surface is large compared to the initial jet thickness, the jet readily attaches to the surface and may be deflected through more than 180° . However, if the radius of curvature is small, the jet turns through a smaller angle, or may not attach to the surface at all. Because size and weight limitations limit the radius of aircraft deflection surfaces, jet deflection angles greater than 60° have been difficult to achieve. Consequently, various techniques have been devised to improve the jet deflection. Von Glahn and Groesbeck (Von Glahn, U. and Groesbeck, D., 1976) used external deflector vanes to turn the jet toward the surface, while Davenport and Hunt (Davenport, F.J. and Hunt, D.N., 1975) used surface mounted director vanes to spread the jet out and reduce its thickness, thus increasing the effective turning radius. They also studied the effect of surface contour, by comparing the deflection of a series of two-piece flaps, which consisted of a circular arc and a straight section. The jet was found to be deflected further by a surface with a small initial radius, followed by a long straight section, than by one with a large initial radius followed by a short straight section.

Several methods of boundary layer control have also been considered. Both Coanda (Metral, Z. and Zerner, F., 1953) and Von Glahn (Von Glahn, U., 1958) studied the effectiveness of multiple flat plate turning surfaces, whose corners were intended to trip the boundary layer and re-energize it. However, not enough data was obtained to show an advantage. Bradbury and Wood (Bradbury, L.J.S., and Wood, M.N., 1965) examined the effect of auxiliary jets along the Coanda surface. These were found to be effective in delaying the separation of subsonic jets, but had no effect on supersonic jets.

Supersonic Coanda jets, which would be used in an aircraft system, present a special problem. The adjustment of the jet to the pressure outside the nozzle involves a system of shock waves which can detach the jet from the Coanda surface. The purpose of this paper is to present the results of a study into the effect of the expansion and turning shocks on the deflection of supersonic Coanda jets, and to describe a nozzle devised to improve thrust vectoring by eliminating this shock system. A combination of analysis and testing has been utilized. In the next section, the phenomena which determine the deflection of Coanda jets are considered in more detail. The design of a new nozzle, devised to test the hypothesis that eliminating the turning shocks will improve the thrust vectoring, is presented in the following section. The test apparatus and the procedures used to measure the jet thrust and turning angle are described in the section after that. In the last section, the test results are presented and analyzed. It is concluded that eliminating the expansion shocks with a convergent-divergent nozzle significantly improves the thrust vectoring compared to the simple convergent nozzles in current use, and that shaping the velocity profile to eliminate turning shocks further improves the thrust vectoring.

COANDA JET DEFLECTION

There are actually two problems in deflecting a jet over small radius curves (generally, those with a radius less than 10 jet thicknesses): that of initially attaching the jet, and that of delaying the eventual separation of the attached jet. The inertia of the jet itself resists its initial attachment. As the radius of the turn decreases, the inertial force, $\rho V^2/R$, becomes larger than the radial pressure gradient, $\partial P/\partial r$, which draws the jet to the surface. At some point, the jet will not attach. Attachment limits have not been established, but the minimum radius of attachment decreased with increasing Mach number. (Bradbury, L. J. S., Wood, M. N., 1965). We believe this is because it becomes more difficult for the jet to adjust to the influence of the Coanda surface: the flow on the lower wall inside the nozzle must accelerate faster than the flow on the upper wall in order to skew the velocity profile and adjust to the radial pressure gradient at the nozzle exit. The radial pressure gradient enables the jet to turn smoothly onto the Coanda surface. In a subsonic jet, this adjustment is made easily, because the effect of the surface curvature can be transmitted upstream into the nozzle. A supersonic jet cannot make this adjustment, so that it has greater resistance to turning.

A jet which has attached to a flat plate will remain attached, in the absence of external disturbances. However, due to the action of viscosity, a jet which has attached to a curved plate will eventually separate. Viscosity causes the development of a boundary layer at the inner edge of the jet and a mixing layer at the outer edge, where the surrounding fluid is entrained. This eventually causes the boundary layer to separate in the following way: as the jet flows around the curved surface, the inertia force is balanced by the radial pressure gradient; that is,

$$\frac{\partial P}{\partial r} = \frac{\rho V^2}{R} \quad (1)$$

as shown schematically in Figure 2. Dimensionally, this equation may be interpreted as

$$\frac{\Delta P}{\delta} = \frac{\rho V^2}{R} \quad (2)$$

in which δ is the thickness of the jet. Thus, to first order, the pressure on the Coanda surface is given by

$$P(\phi) = P_{\infty} - T(\phi)/R(\phi) \quad (3)$$

in which $T = \rho V^2 \delta$ is the local momentum of the jet and ϕ is the angular position along the surface. As the jet flows around the surface, its thrust is reduced by wall friction and the average radius of curvature, R , is increased by mixing with the surroundings. Both these effects cause the surface pressure to rise. The jet boundary layer eventually separates in the resulting adverse pressure gradient. Of course, the boundary layer may separate sooner, if a more severe gradient is imposed on it, as by an impinging shock wave or an increase in surface curvature.

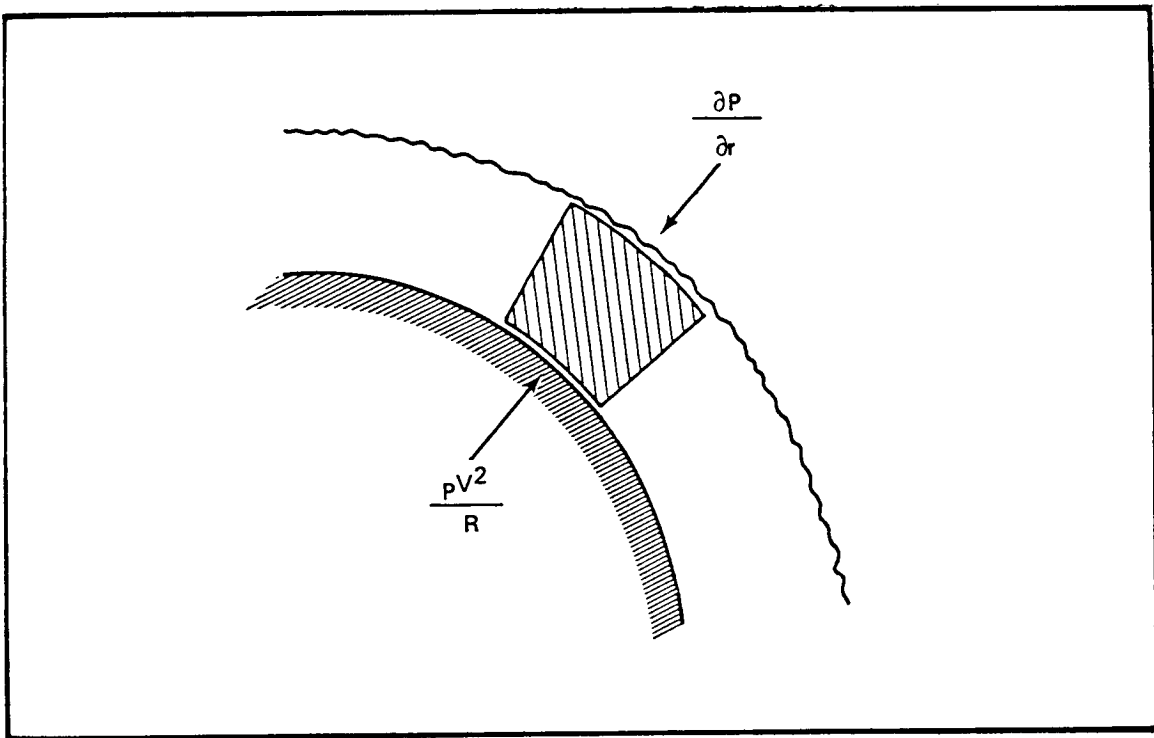


Figure 2. Radial force balance in a Coanda jet segment

There are no theories for predicting the point of separation. But, if it is assumed that the separation angle depends on the initial thrust of the jet, the radius of the Coanda surface, and the properties of the fluid, dimensional analysis gives

$$\phi_{\text{sep}} = \phi(R/t, Re, M) \quad (4)$$

Re and M are the jet Reynolds number and Mach number, respectively. The form of this function can be determined from experimental data. Although not enough data has been obtained to do so, the value of this function has been determined in some

limiting cases: for incompressible flow ($M = 0$), Newman (Newman, B.G., 1961) found that the separation angle increases with R/t and Re to a maximum value of about 245° . At $R/t = 5$, the turning angle is about 170° . In the transonic regime, Davenport and Hunt (Davenport, F.J., and Hunt, D.N., 1975) did not obtain more than 100° of turning, and achieved only about 60° at $R/t = 5$. There is very little data for supersonic Coanda jets, but Bradbury and Wood (Bradbury, L.J.S., and Wood, M.N., 1965) found that the separation angle decreases as the Mach number is increased. All these data were obtained with convergent nozzles.

The system of expansion shocks which adjusts the jet from a convergent nozzle to the exit pressure may be eliminated by using a convergent-divergent nozzle. It seems reasonable to expect that this would improve the jet turning by eliminating shock-induced boundary layer separation. However, such a jet would still resist the initial attachment, because the radial pressure gradient is zero at the nozzle exit. Even if the entrainment is strong enough to attach the jet, the system of expansion waves which then develops may cause it to separate again within a short distance. The wave system is sketched in Figure 3. The expansion waves which are formed when the jet deflects onto the surface are reflected from the outer jet boundary as a system of compression (shock) waves. These compression waves then impinge on the jet boundary layer. If the impinging shock is strong enough, the jet will separate from the surface at this point.

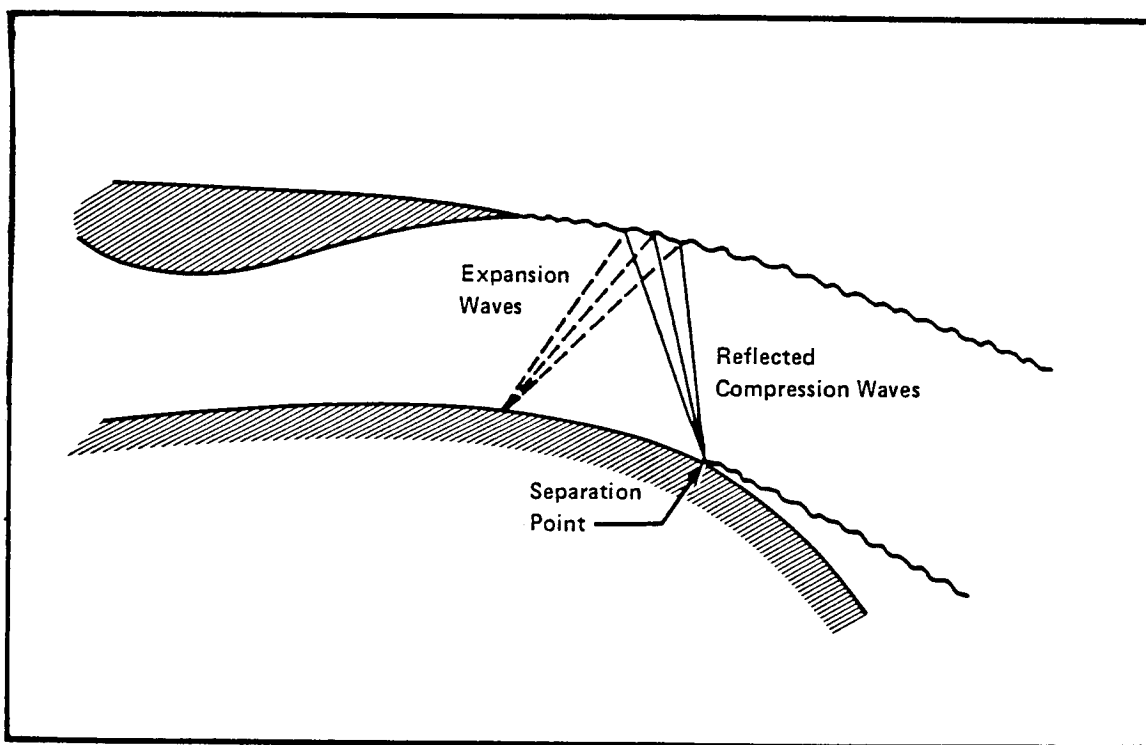


Figure 3. Jet Detachment due to Wave Interaction

A convergent-divergent nozzle can be designed to produce a skewed velocity distribution. If the high velocity, low pressure side is on the surface, the radial pressure gradient will act to deflect the jet in that direction. In fact, by suitable shaping of the velocity profile, the jet deflection can theoretically be matched to the curvature of the Coanda surface. For example, the streamlines of an irrotational vortex flow are circular, and the velocity varies inversely with distance from the center of rotation, $V = K/R$. A jet having such a velocity distribution can be matched to the radius of a circular Coanda surface, and should flow around that surface without turning losses due to expansion waves, Figure 4. One objective of our study was to evaluate the hypothesis that shaping the jet velocity profile improves the thrust vectoring of supersonic Coanda jets. This was accomplished by designing a convergent-divergent nozzle which produces a skewed velocity profile, and then comparing its turning angle and thrust to those of a simple converging nozzle and a conventional convergent-divergent nozzle.

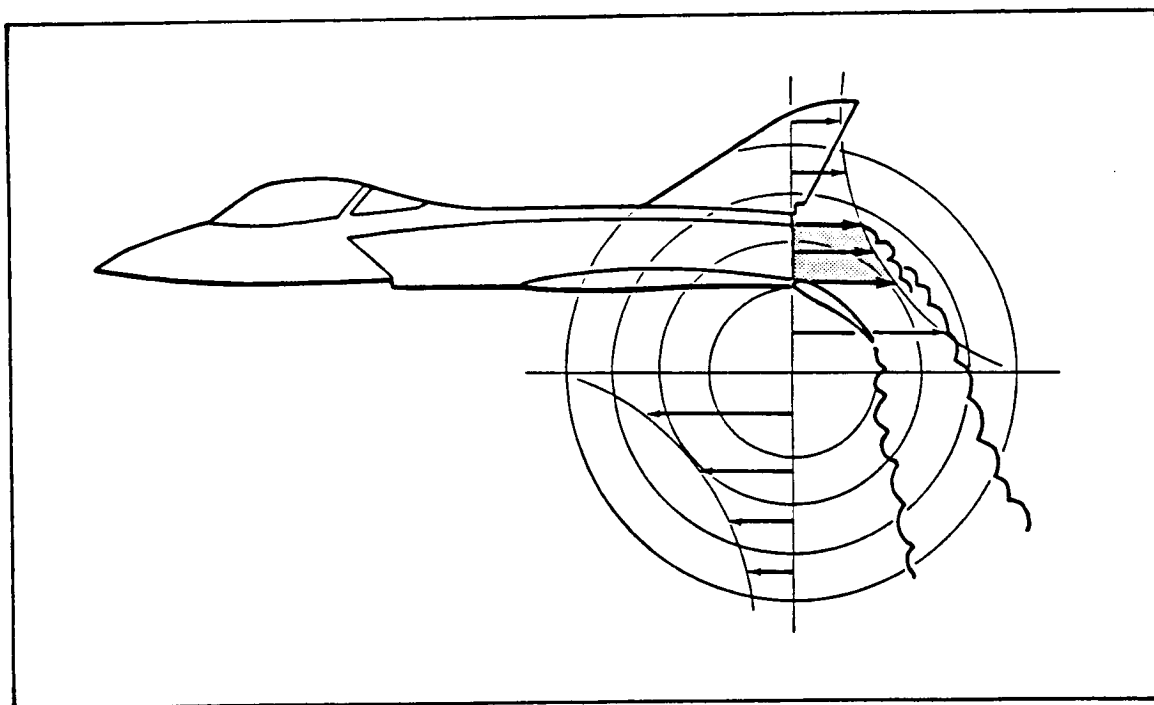


Figure 4. Jet Velocity Distribution Matched to a Circular Coanda Surface

NOZZLE DESIGN PROCEDURE

Method of Analysis

Although a method of designing nozzles which deliver a vortex velocity profile ($V = K/R$) was developed by Guile (Guile, B.G., 1961) for his work on aerodynamic windows, it was felt a more flexible procedure was needed for our Coanda jet application. Guile's method involves first expanding the flow to some uniform Mach number, and then expanding the flow further in order to skew the velocity profile. Such a two-stage design procedure results in a nozzle which is too long for most aircraft systems. Further, this approach constrains the shape of the

exit velocity profile, which then constrains the shape of the Coanda surface. Therefore, a method of designing a single-stage nozzle which delivers an arbitrary exit velocity profile was developed for this study.

Consider a nozzle discharging a supersonic jet onto a curved surface, as sketched in Figure 5. If the jet turns isentropically, the governing equations are hyperbolic, so that the nozzle velocity profile must satisfy the compatibility relations on the network of characteristics which connect the nozzle exit to the jet boundaries. In this sense, the curvature and Mach number at the jet boundaries determine the velocity profile at the nozzle exit. The relevant sections of the boundary appear to be ZA and YB; however, conditions along YB are influenced by the free boundary segment XZ, as well as by the shape of YB. Thus, the velocity profile is determined by the shape of the wall along YB and the shape and Mach number along XA.

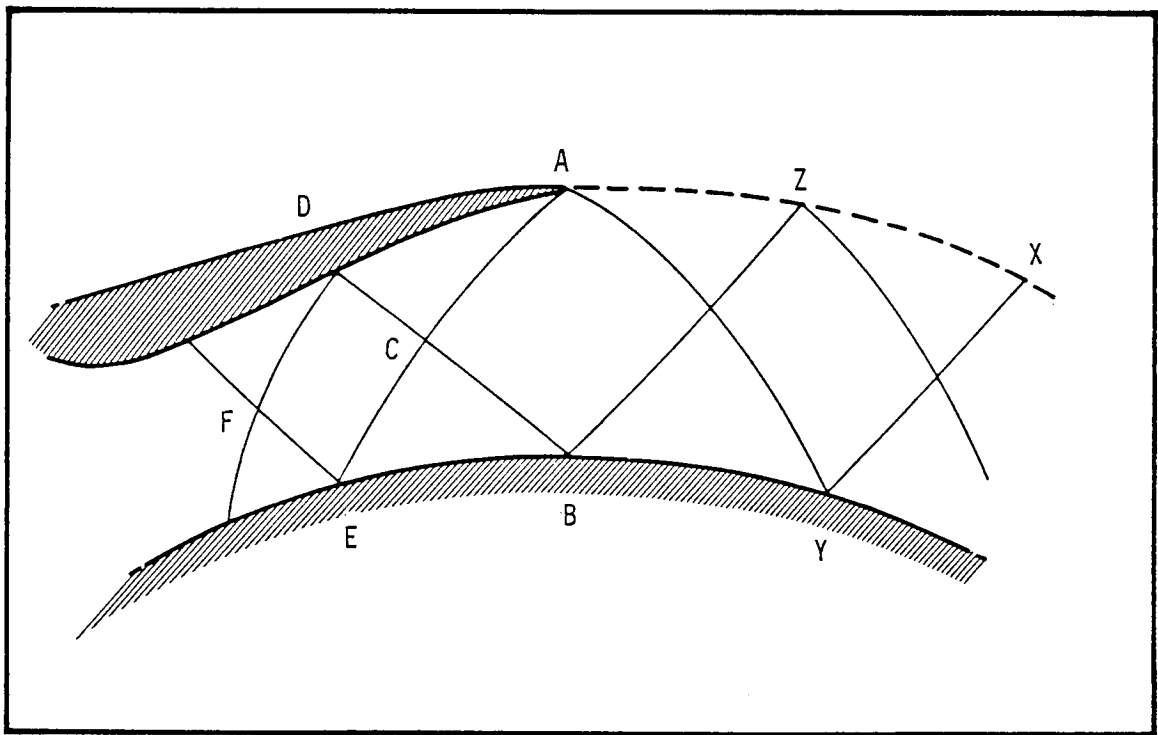


Figure 5. Characteristics Net of a Supersonic Coanda Jet

The method of characteristics (Liepman, H. W. and Roshko, A.) may be used to calculate the initial velocity profile which matches the Coanda jet to a particular surface. The method is based on satisfying the compatibility relations, $\theta \pm \nu(M) = \text{constant}$, between the Prandtl-Myer function, ν , and the flow angle, θ . To determine the initial velocity profile, a characteristics net is run upstream from the jet boundaries. For example, if the Mach number at point Z is $M = 1.5$ (corresponding to $\nu = 12^\circ$) and the flow angle is $\theta = -10^\circ$, then the compatibility constant on the left running characteristic through point B is $12^\circ - (-10^\circ) = 22^\circ$. Since the angle at point B is defined to be $\theta = 0^\circ$, the compatibility relation gives $\nu = 22^\circ$, which corresponds to a Mach number of 1.8. The Mach number distribution of the inviscid flow along YB may be determined in this way. The Mach number profile at the nozzle exit is similarly determined by the intersecting characteristics from ZA and YB.

The internal contours of the nozzle which will produce the desired velocity profile may be computed by continuing this solution procedure upstream into the nozzle. The shape of the zone ABC and the flow within it are determined by the characteristics from the exit profile; outside this zone the flow is influenced by the wall contours. A wide range of contours can be defined which yield the goal upstream of uniform flow at $M = 1$ (a nozzle throat). Guile's method (Guile, R.N., 1975) yields one such contour; our one-step method yields other shapes.

Because the range of possible contours is so large, our basic procedure is to define an approximate shape using the coarse net of characteristics from the points AB and MN, as shown in Figure 6. This shape is then developed using a fine-net operator. The region ABKLJ is an expansion zone for the jet, but it is designed as a compression zone for a fictitious flow which goes backwards through the nozzle. This region contains both left- and right-running characteristics which are curved. The regions JLM and KLN are cancellation zones designed to eliminate the compression waves generated in the region ABKLJ. Thus, these are simple regions containing waves of only one family. In the region LMN the flow is uniform and parallel, at the throat Mach number (e.g., $M = 1.001$).

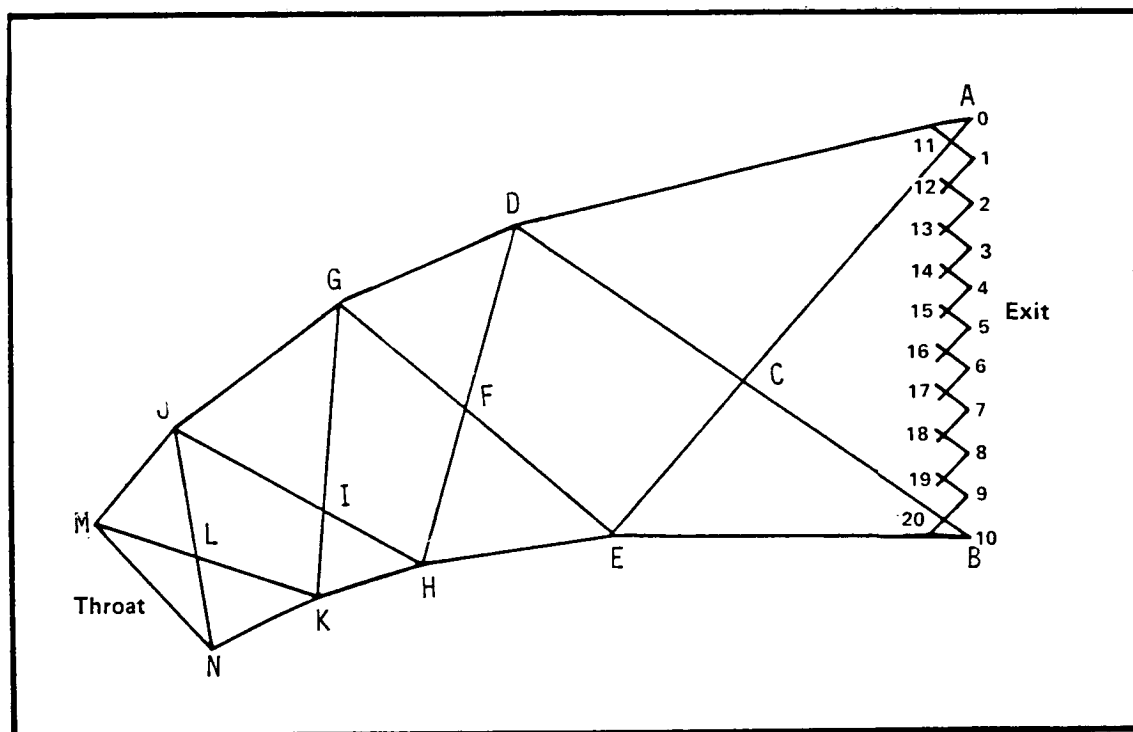


Figure 6. Coarse and Fine Net Operators for Nozzle Design

To define the coarse net, the Mach number and flow direction at Point I are specified, and the coarse net is then analyzed for compatibility. For example, the conditions at Point G are related to those at A through the Point E and to those at M through the Point K. The Mach numbers on the walls of a "suitable" coarse net increase monotonically from the throat to the exit. The conditions at Point I are varied until a suitable coarse net is defined. The nozzle flow is then calculated in detail by marching upstream from the nozzle exit using a fine characteristics net. The wall conditions are then examined to insure that the Mach number distribution is satisfactory. If necessary, the coarse net is modified and the fine net analysis is repeated. The integral method of boundary layer analysis devised by Dayman (Dayman, B., 1963) was used to correct the inviscid nozzle contours for the boundary layer displacement thickness. Details of the nozzle design procedure and computer code are given by Bevilaqua and Lee (Bevilaqua, P. M. and Lee, J. D., 1980).

The initializing mesh points and the starting profiles at the nozzle exit for the vortex nozzle and the baseline uniform flow nozzle tested in this study are shown in Figure 7. The nozzles were designed to deliver these profiles. The same subsonic section was added to the upstream end of both nozzles. The subsonic section is a simple cubic surface having both first and second derivatives going to zero at the throat. Both nozzles are shown in Figure 8.

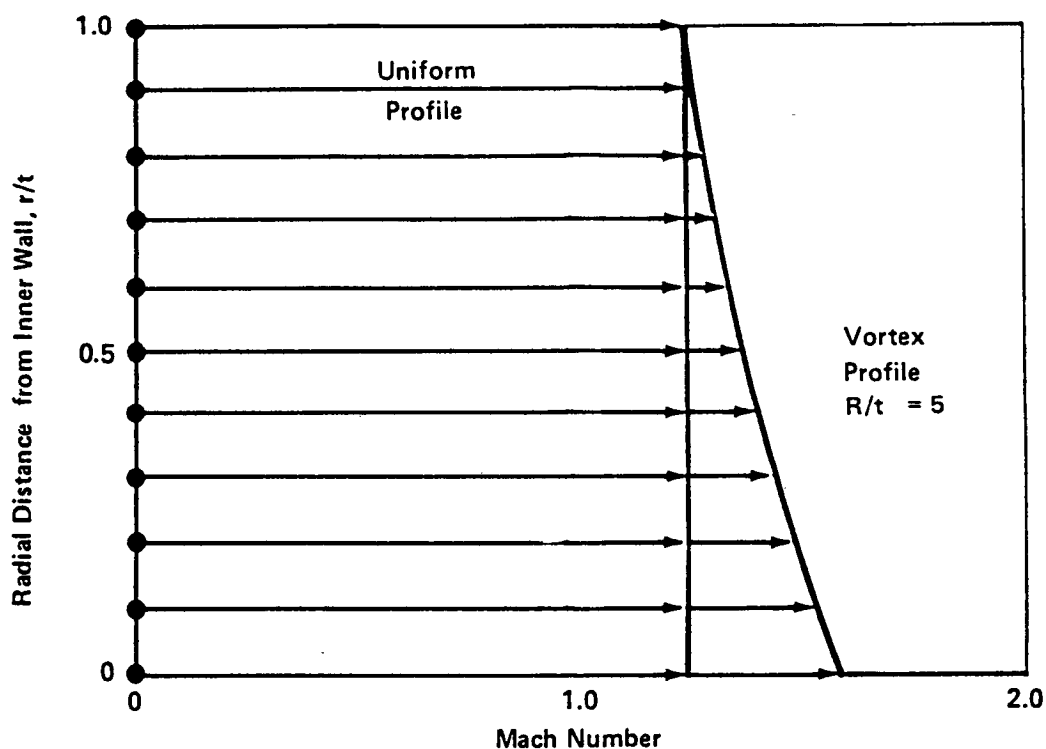


Figure 7. Uniform and Skewed Nozzle Exit Velocity Distributions

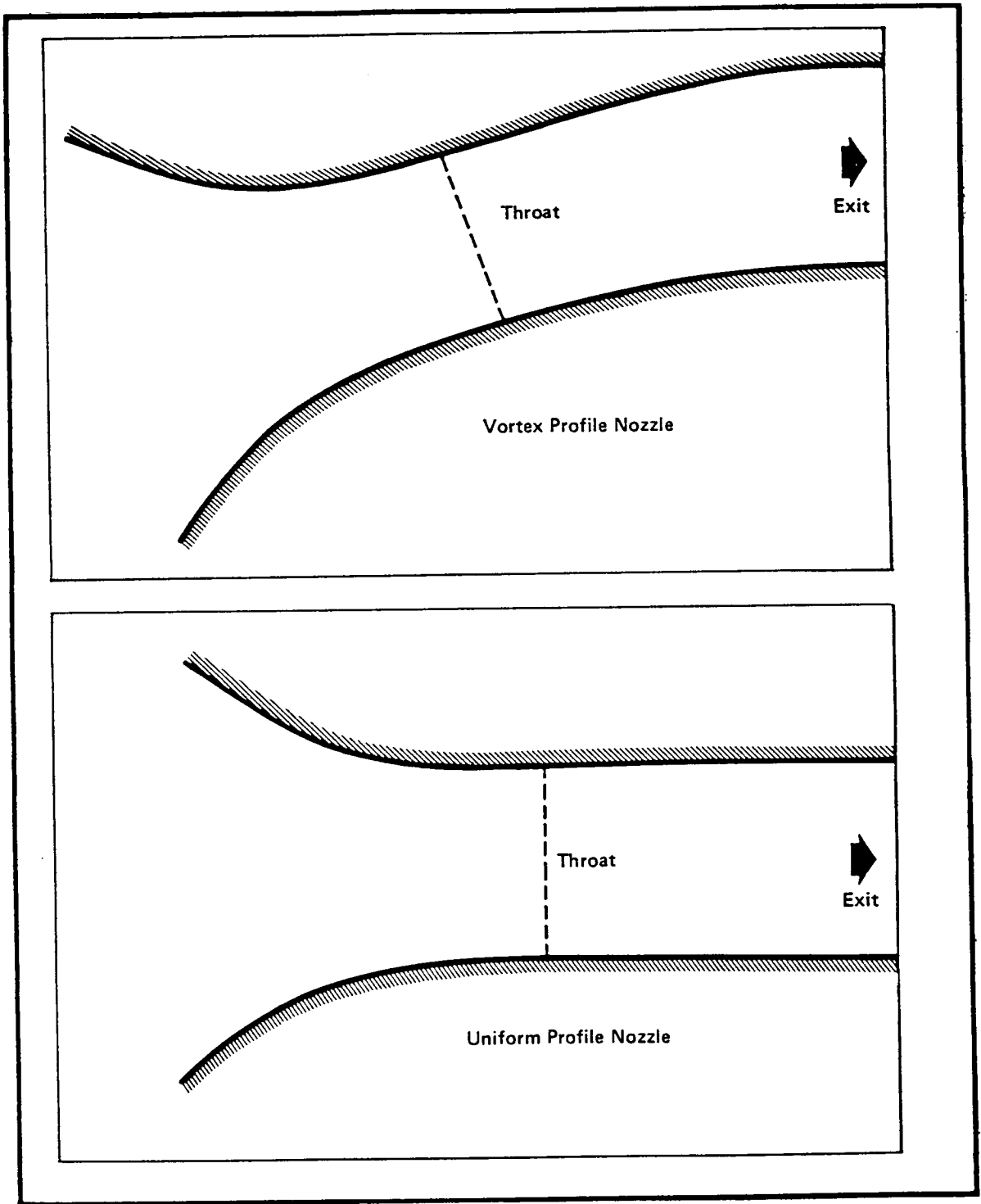


Figure 8. Contours of the Convergent-Divergent Nozzles

Description of the Model

The model consisted of a steel plenum box on which interchangeable nozzle and Coanda surface assemblies could be mounted, as shown in Figure 9. This plenum was attached to the balance post and connected to the air supply hoses with two four-inch pipes. A pressure tap in the plenum sidewall was used to measure the plenum pressure. Provisions were made to mount air distribution baffles in the plenum, but it was found that none were needed.

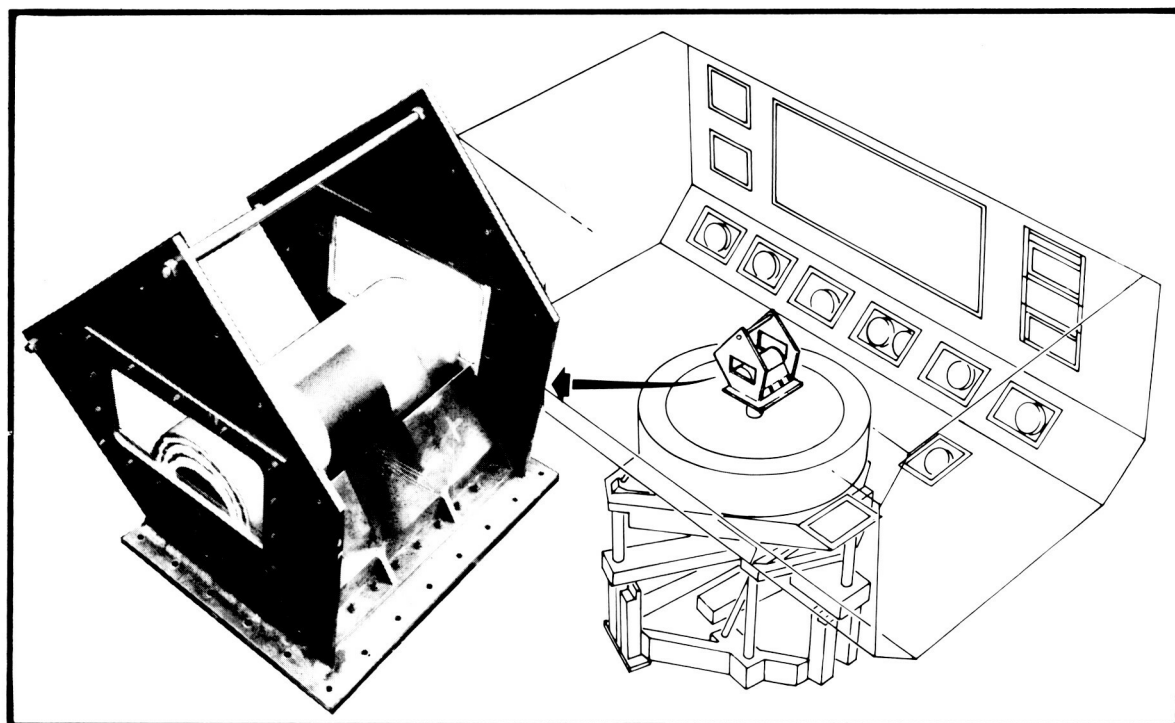


Figure 9. Coanda Jet Nozzle Test Assembly

Both nozzle assemblies were nominally identical except for the nozzle contours. Each assembly consisted of aluminum nozzle and Coanda surfaces mounted between steel endwalls. The nozzles had a span of 30.5 cm and nominal exit dimensions of 1.27 cm. The circular Coandas had a radius of 6.35 cm, giving $R/t = 5$. Both endwalls had openings which could be fitted with optical glass windows for flow visualization or with steel inserts for the force data runs. When the windows were not installed, the nozzle assembly was fitted with endwall boundary layer splitter plates. These splitter plates were 1.5 mm thick. These were mounted 1.27 cm and 2.54 cm from each endwall and were intended to insure the two-dimensionality of the flow by removing the corner vortices. This technique was developed by Guitton and Newmann (Guitton, D. E., Newman, B. G., (1977).

The entire nozzle assembly was bolted to the plenum such that the nozzle exit plane was 45° from the horizontal with the jet exhausting upward. Each nozzle assembly was instrumented with fifteen pressure taps located on the inside nozzle contours and every 30° along the Coanda surface at midspan.

The model was tested in the 7' x 10' test section of the North American Aircraft low speed wind tunnel in Columbus, Ohio. The plenum was attached to a post connected to the six component external pyramidal balance. The model air supply was brought through two venturis and cono-flow control valves. Two four-inch flexible hoses were used to bridge the balance with a minimum of interference.

Instrumentation

Model forces were measured by the external six-component balance. The air supply mass flow was measured by two venturis in which the supply pressure, differential pressure, and temperature were measured. The nozzle exit total pressure was calibrated versus the model plenum pressure which was obtained from the plenum wall static tap. Model surface pressures were recorded using a scanivalve. The air supply hose pressure was measured to be used for computing hose tares. All instrumentation was calibrated and read through the wind tunnel data system. The data was recorded and reduced by an IBM 1800 data acquisition computer. Nozzle exit and jet profile survey data were acquired on an x-y recorder using a pressure transducer and a calibrated traverse position potentiometer.

RESULTS AND DISCUSSION

Convergent Nozzle

In order to provide a baseline for evaluating the performance of the convergent-divergent nozzles, the jet from a simple converging nozzle was tested first. The measured variation of the jet thrust coefficient and deflection angle are shown in Figures 10 and 11. These were determined from the measured vertical and horizontal components of the force according to the relations $T = (F_V^2 + F_H^2)^{1/2}$ and $\phi = \tan^{-1}(F_V/F_H)$. The thrust deflection angle is not the same as the jet separation angle, because the mixing of the jet with the surrounding fluid causes the outer jet boundary to turn more slowly than the inner boundary. As a result, the thrust vector is not tangent to the surface at the separation point.

In Figure 10, it can be seen that the attachment and detachment of the jet shows some hysteresis in the range of pressure ratios between 2.0 and 2.6; that is, the jet remains attached as the pressure ratio is increased through this range, and remains detached as it is decreased through this range. Perhaps more surprising is the magnitude of the angle through which the jet was deflected. The maximum deflection of almost 145° is nearly two and a half times that achieved by Davenport and Hunt (Davenport, F.J. and Hunt, D.N., 1975). Thus, it seems possible that the straight section which they added to the Coanda surface actually caused premature separation of the jet by inducing a sudden increase in the surface pressure gradient.

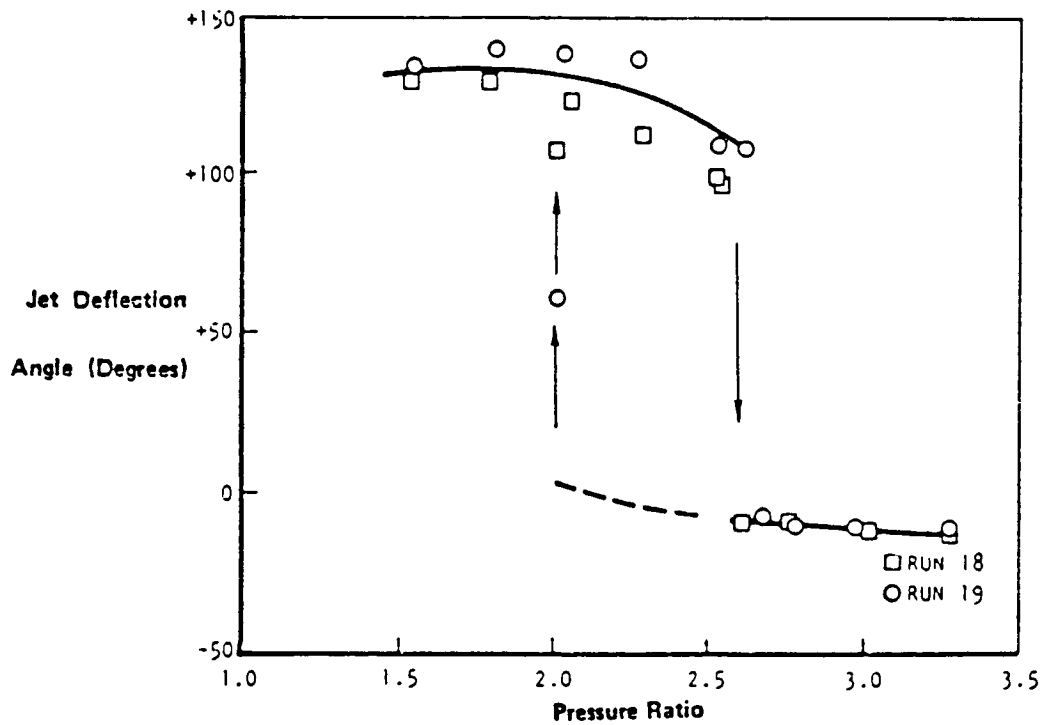


Figure 10. Converging Nozzle Thrust Coefficient

The variation of the jet thrust coefficient is shown in Figure 11. This coefficient is defined as the ratio of the measured jet thrust to the thrust calculated for an isentropic expansion of the measured nozzle mass flow to atmospheric pressure. When the jet is attached to the Coanda surface, its thrust is reduced by wall friction. As seen in the figure, this loss can be significant for large jet turning angles.

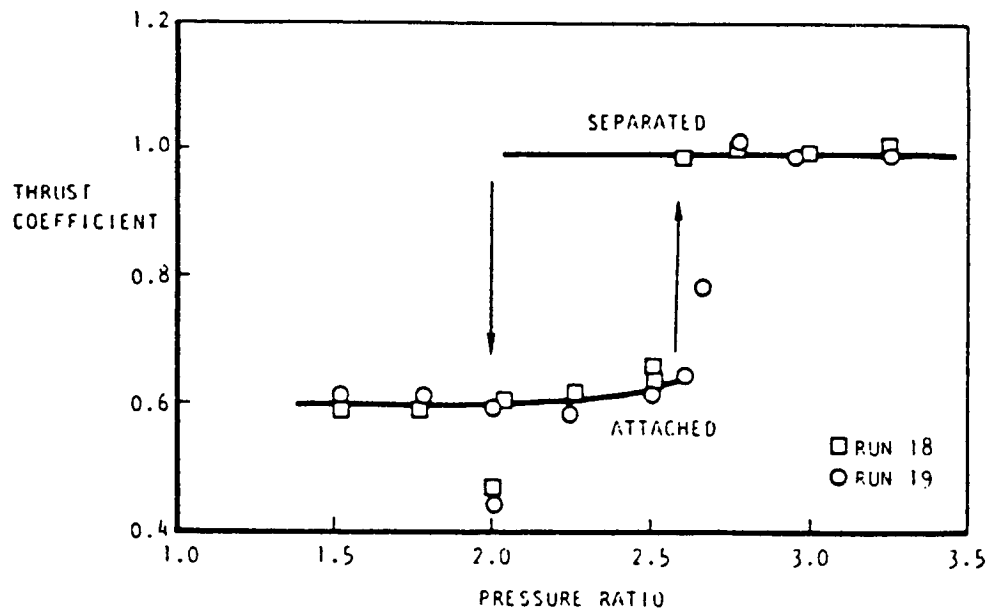
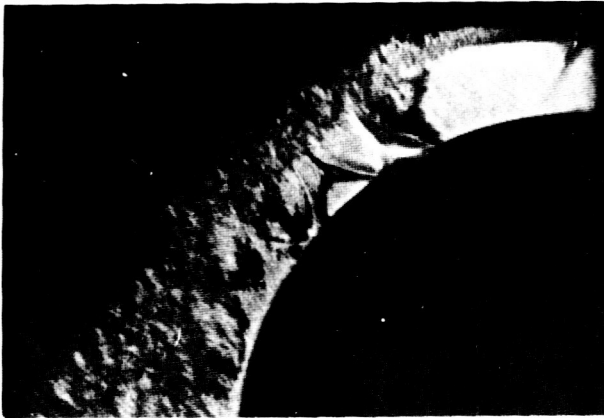
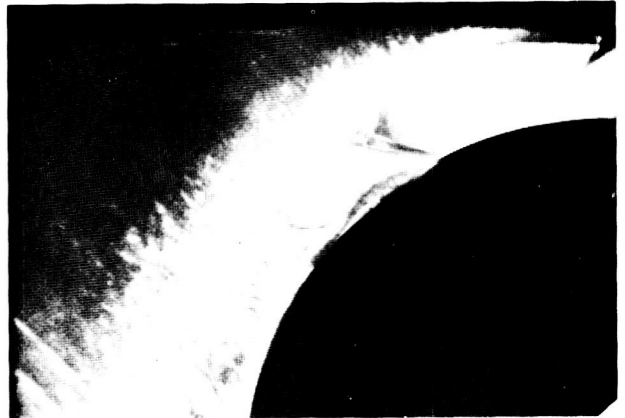


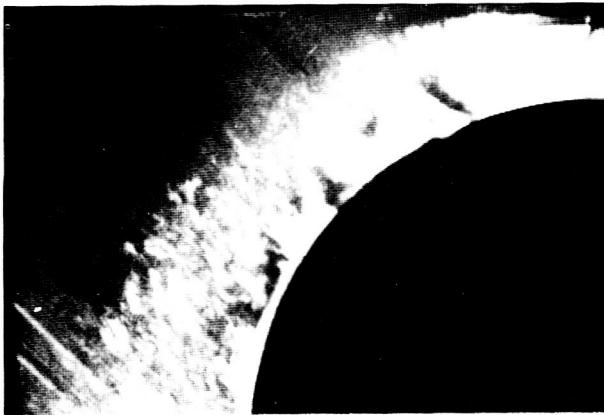
Figure 11. Converging Nozzle Jet Deflection



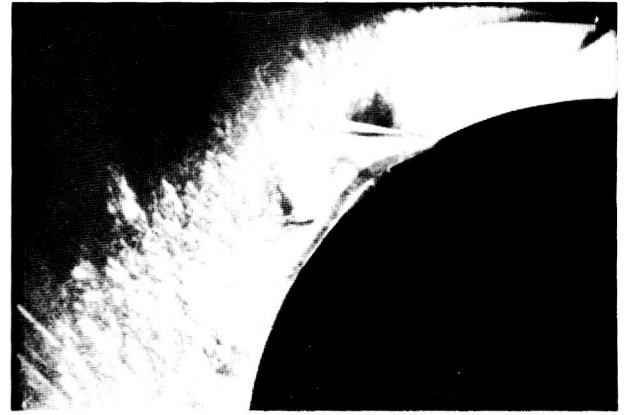
PR~2.25



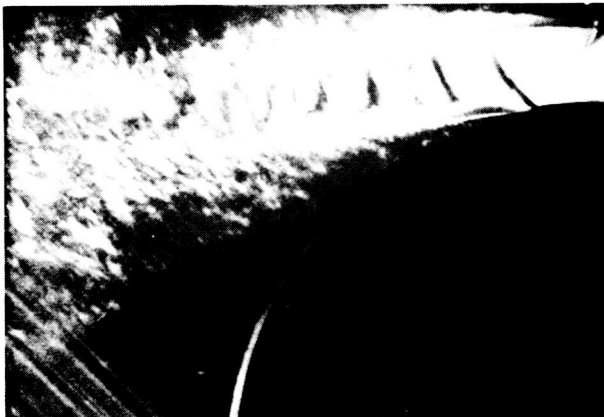
PR~2.5 ATTACHED



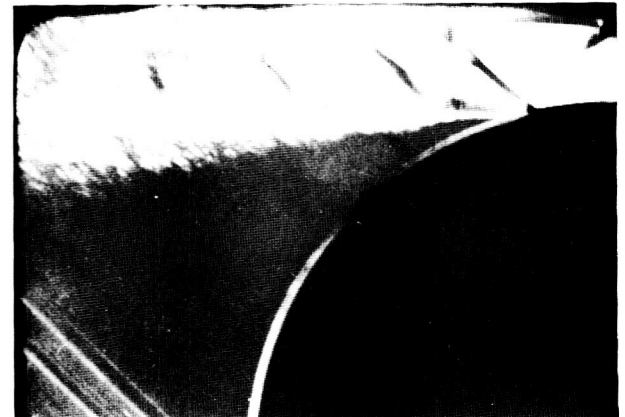
PR~2.0 AFTER REATTACHMENT



PR~2.65 BEFORE DETACHMENT



PR~2.0 BEFORE REATTACHMENT



PR~2.65 AFTER DETACHMENT

Figure 12. Schlieren Photographs of the Jets from the Convergent Nozzle

As an aid in understanding the behavior of the jet, Schlieren photographs were made of the region downstream of the nozzle exit. In Figure 12, it can be seen that detachment of the jet is caused by shock induced boundary layer separation. As the pressure ratio is increased, the first compression wave reflected from the wall can be seen to strengthen, so that the separation bubble behind it becomes larger. Eventually, the wave system becomes strong enough to completely separate the boundary layer and thus detach the jet. The separation point of the detached jet is closer to the nozzle than the initial separation point. If the pressure ratio is subsequently reduced, the jet can be seen to deflect slightly towards the wall, although it does not immediately reattach to the surface.

Convergent-Divergent Nozzles

For both convergent-divergent nozzles, surface pressure distributions and total pressure distributions were measured, in addition to the force data and Schlieren photographs, in order to verify the nozzle performance. In Figure 13, the pitot pressure profile at the exit of the vortex nozzle is compared to the predicted distribution. Since the local Mach number is higher near the inner wall, the loss of total pressure due to the probe shock is larger there. Thus, the slope of the total pressure profile is opposite to the slope of the velocity profile. The agreement between measurement and prediction is very good, which indicates that the desired skewing of the exit velocity profile was achieved. The spike in the profile at the inner boundary was also seen in the uniform profile from the conventional convergent-divergent nozzle, which suggests that probe interference may be the cause.

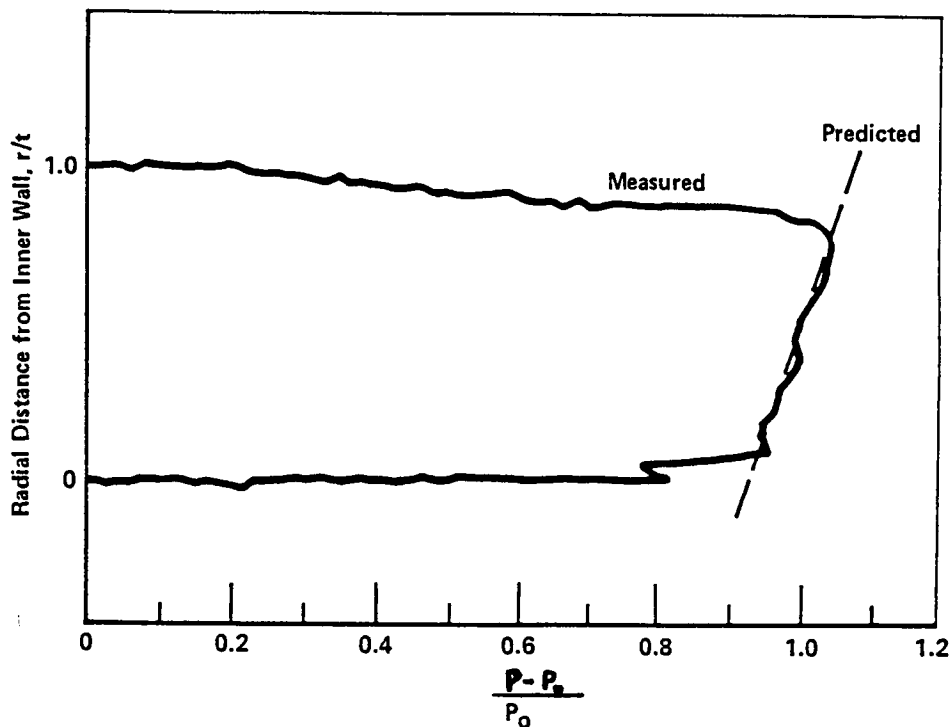


Figure 13. Vortex Nozzle Total Pressure Profiles

In Figures 14 and 15, the measured nozzle wall static pressure distributions are compared to the design pressure distributions. The agreement is very good for the uniform profile nozzle. However, a pressure tap on both the upper and lower surfaces of the vortex profile nozzle falls off the design distribution. Since these taps show similar pressure variations at subsonic pressure ratios, it is likely that they are defective, but it is also possible that a compression wave originates on the upper surface of the nozzle where the pressure gradient is relatively flat. If such a wave exists, it is weak, since the desired total pressure distribution was observed at the nozzle exit.

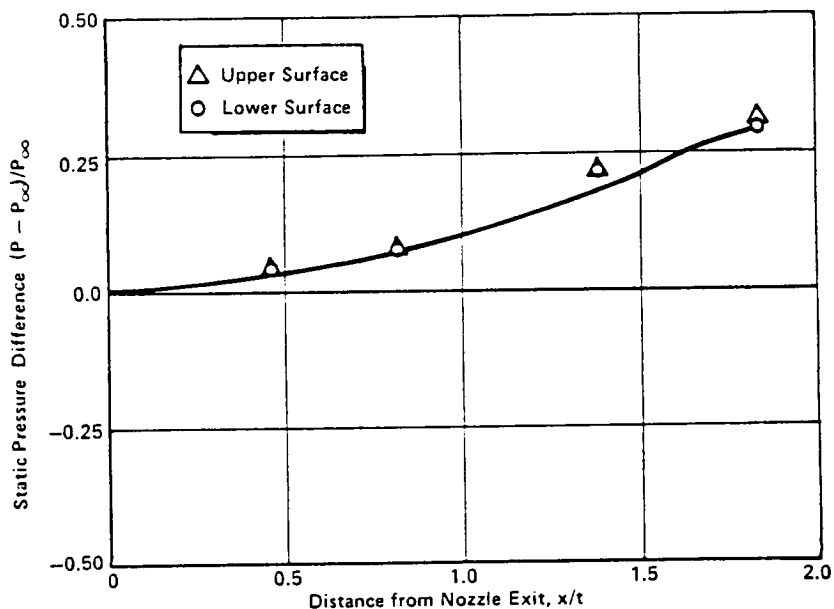


Figure 14. Surface Pressures in the Symmetric Nozzle

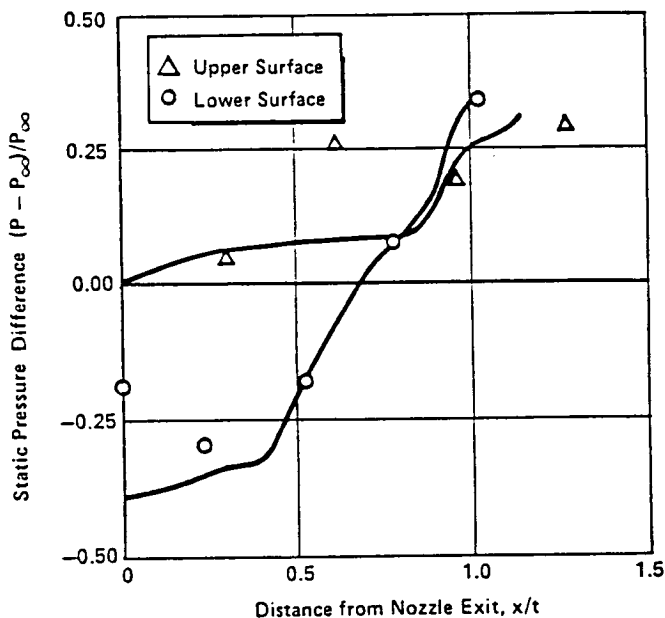


Figure 15. Surface Pressures in the Vortex Nozzle

The static pressure distributions on the Coanda surface at the design pressure ratio of 2.5 are shown in Figures 16 and 17. In both figures, the nozzle exit is at the top. There are 5 equally spaced taps between the throat and the exit of each nozzle, and a tap every 30° along the Coanda surface. The general shape of the measured pressure distributions are similar for both nozzles. As the flow expands through the nozzle, the pressure decreases to atmospheric pressure. Then, as the jet is turned onto the Coanda surface, the pressure drops well below atmospheric pressure. Viscous effects then cause it to increase again.

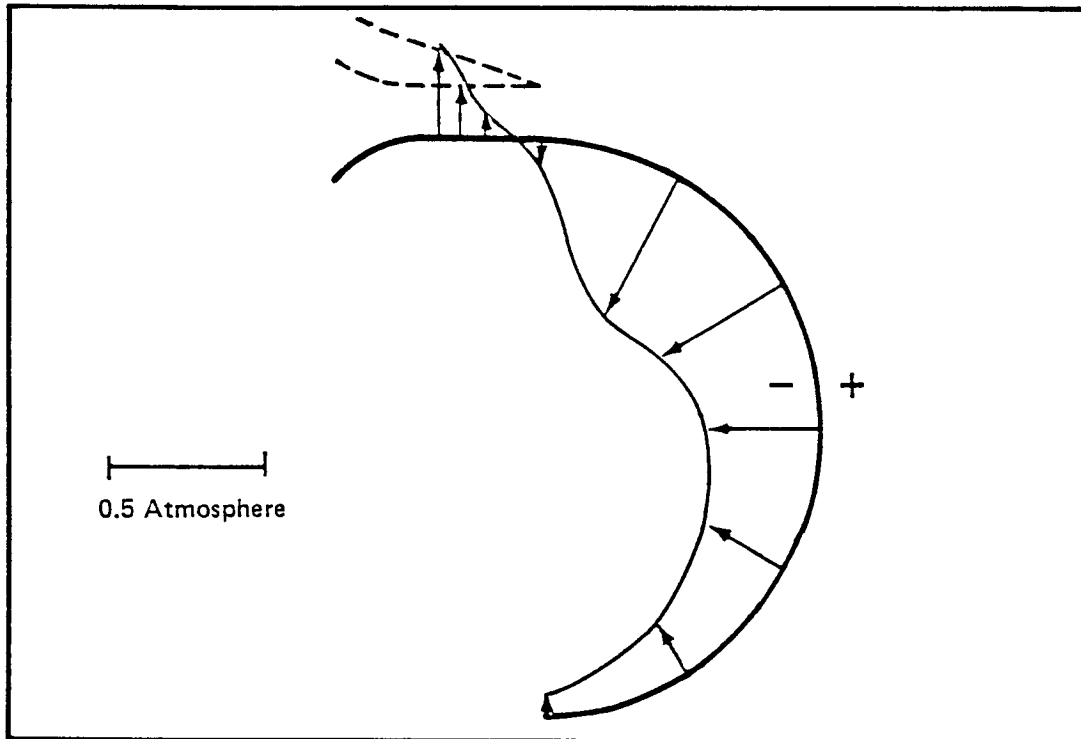


Figure 16. Surface Pressures Outside the Symmetric Nozzle

The pressure on the upper wall of the convergent-divergent nozzle decreases smoothly to atmospheric pressure, as expected. On the lower wall, however, the pressure at the exit is slightly below atmospheric pressure, as seen in Figure 16. This may be due to the formation of a separation bubble, which develops because the jet resists turning, and attaches downstream of the nozzle exit.

The surface pressure under the Coanda jet can be estimated using Equation 3. The jet thrust was calculated from the measured mass flow, \dot{m} , and the nozzle pressure ratio, according to the relation

$$T = \left[\dot{m} \frac{2\gamma}{\gamma-1} R T_0 \left(1 - (P_\infty/P_0)^{1/\gamma} \right) \right]^{1/2}$$

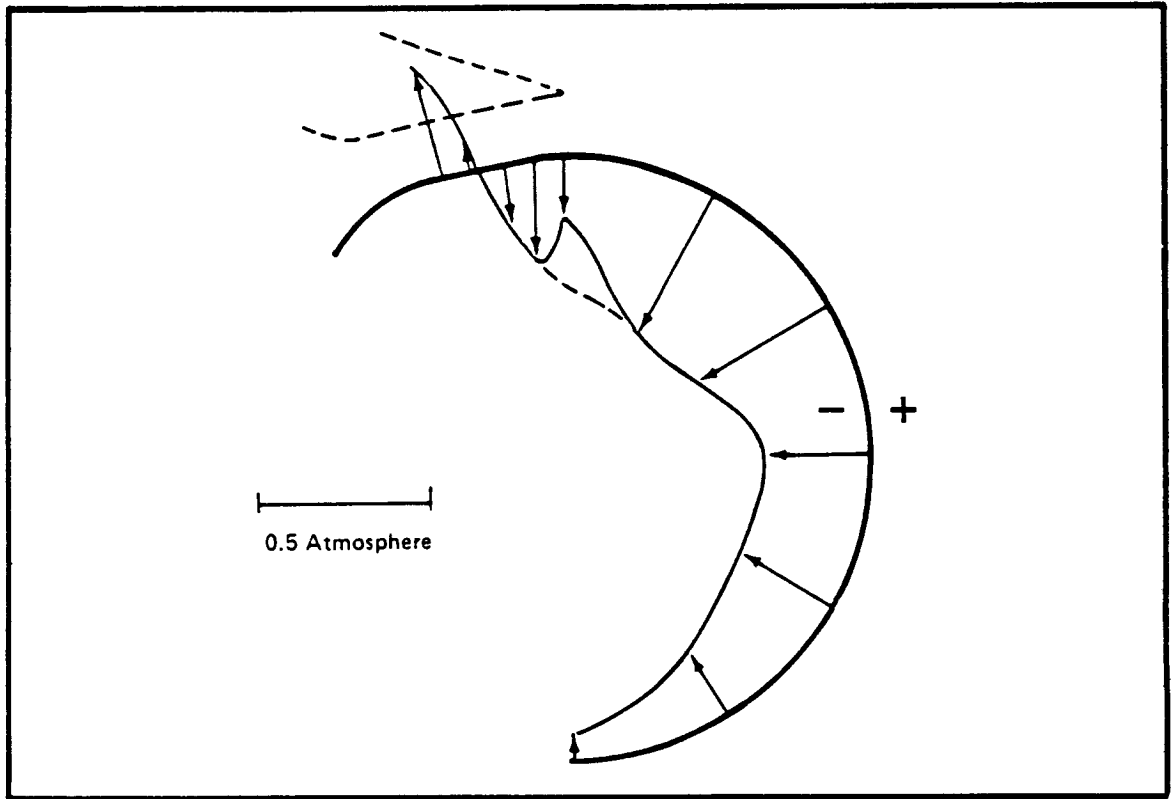


Figure 17. Surface Pressures Outside the Vortex Nozzle

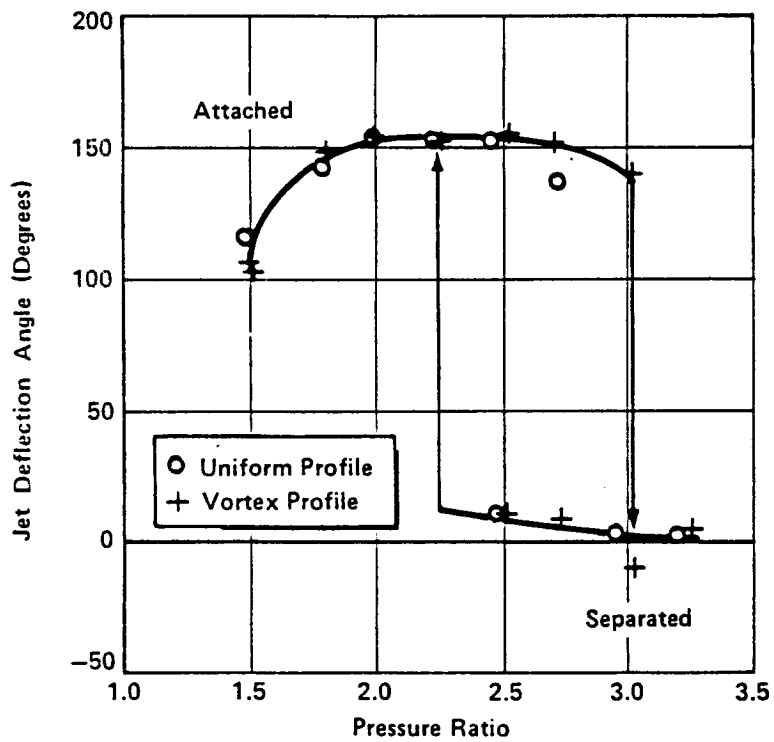


Figure 18. Convergent-Divergent Nozzle Jet Deflection

in which R is the gas constant, while P_0 and T_0 are the stagnation pressure and temperature. At the design pressure ratio, the thrust of the jet is about 27 newtons/cm of span, and the computed pressure drop is 0.39 atmospheres. The lowest pressure measured on the Coanda surface (at $\phi = 30^\circ$) is essentially the same. In Figure 17, the pressure on the inner wall of the vortex nozzle is seen to decrease more rapidly than in the uniform profile nozzle. It approaches the value required to turn the jet at the nozzle exit, as intended.

The measured variation of the jet thrust coefficient and deflection angle are compared in Figures 18 and 19. The attachment and detachment of the jets show some hysteresis for these nozzles also. However, the pressure ratio range for hysteresis, from 2.2 to 3.0, is higher than for the convergent nozzle, and the jet deflection angle, almost 155° , is higher than for the convergent nozzle. In fact, the turning of both jets was probably limited by interference with the nozzle plenum on the back side of the Coanda surface, and not by separation from the Coanda surface.

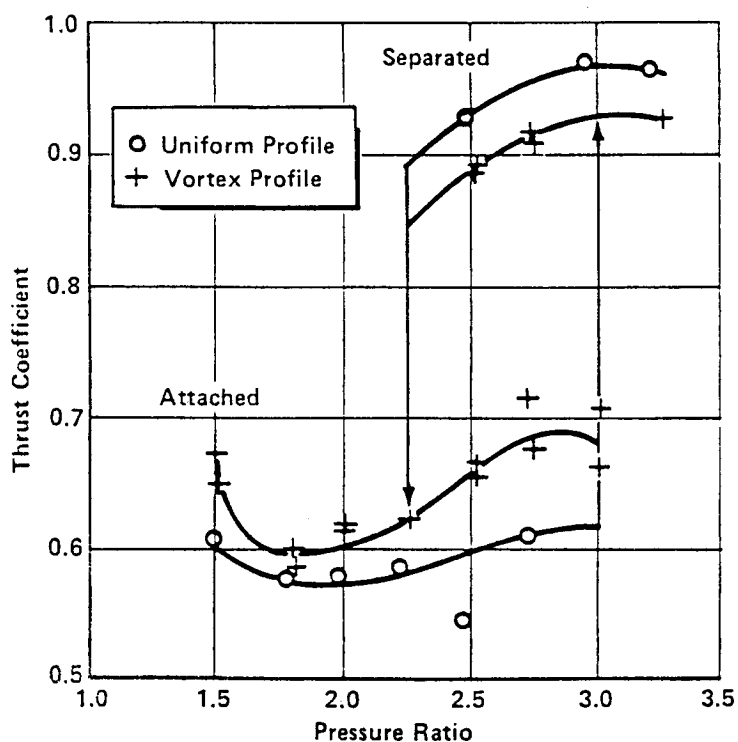
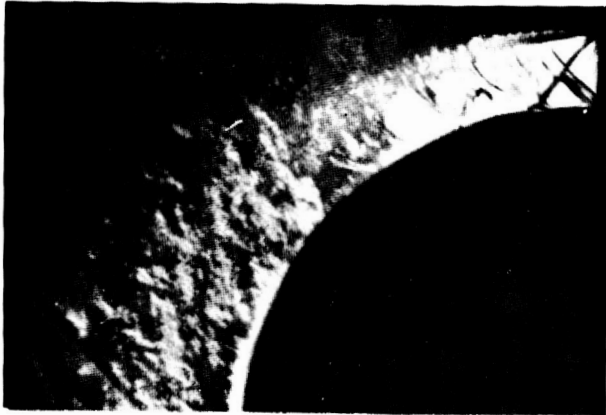


Figure 19. Convergent-Divergent Nozzle Thrust

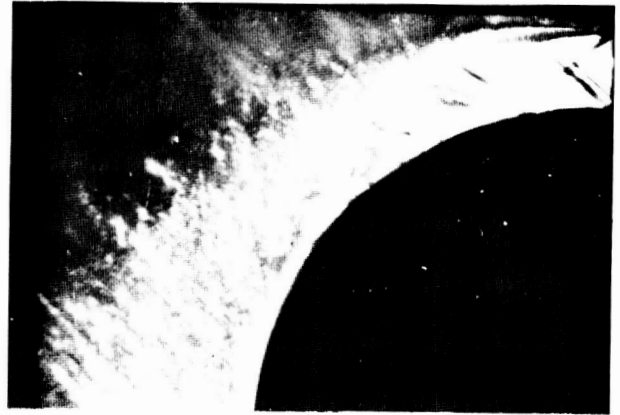
The variation of the thrust coefficient seen in Figure 19 is consistent with the observed deflection of the jet. Initially, as the pressure ratio increases, the jet deflection increases and its thrust is reduced. Then as the pressure ratio increases past the design value of 2.5, the deflection decreases and the thrust correspondingly increases. After detachment, decreasing the pressure ratio causes the jet to deflect toward the surface and the thrust to decrease slightly.

The reason for the difference in the pressure ratio for detachment of these two jets, as compared to the jet from the converging nozzle, may be deduced from the Schlieren photographs in Figures 20 and 21. At the design pressure ratio of 2.5, the first expansion wave is not present in the jets from either convergent-divergent nozzle. Similarly, the turning waves in the jet from the conventional convergent-divergent nozzle are not strong enough to produce a separation bubble. However, by a pressure ratio of 3.0, both jets are sufficiently underexpanded that the expansion wave system does appear. A separation bubble is apparent in this case, and the jets do detach at a slightly higher pressure ratio.

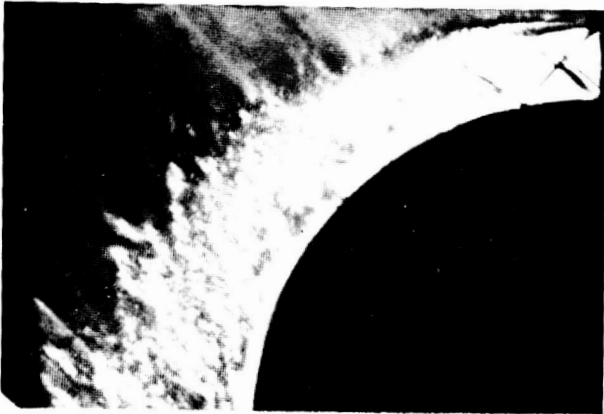
The spreading of the jets is shown by the development of the total pressure profiles in Figures 22 and 23. Both jets develop in the same way. The inner boundary layer and the outer mixing layer have merged by the 30° station to form the total pressure profile typical of wall jets. However, the spreading of these jets is considerably more rapid than that of a wall jet on a flat plate. Also, the jet from vortex nozzle spreads noticeably slower than the jet from the conventional nozzle.



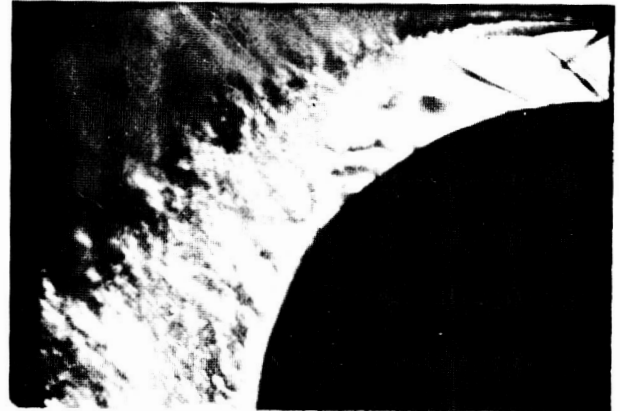
PR~2.0



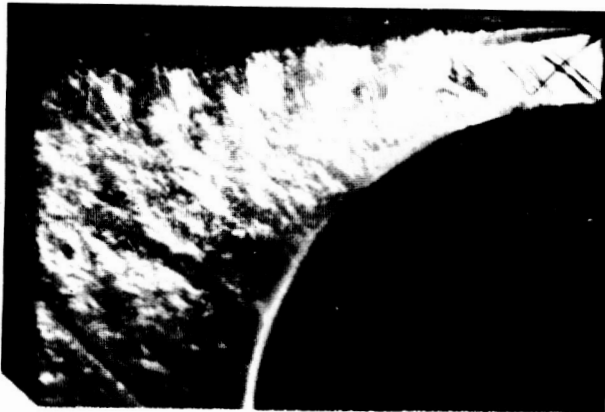
PR~2.5 DESIGN POINT



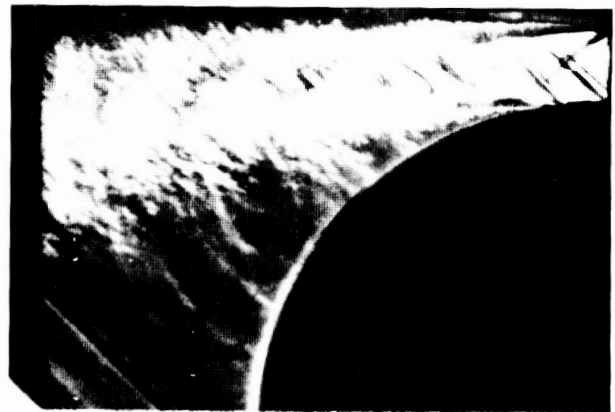
PR~2.25 AFTER REATTACHMENT



PR~2.8 BEFORE DETACHMENT



PR~2.25 BEFORE REATTACHMENT



PR~3.0 AFTER DETACHMENT

Figure 21. Schlieren Photographs of the Jets from the Vortex Profile Nozzle

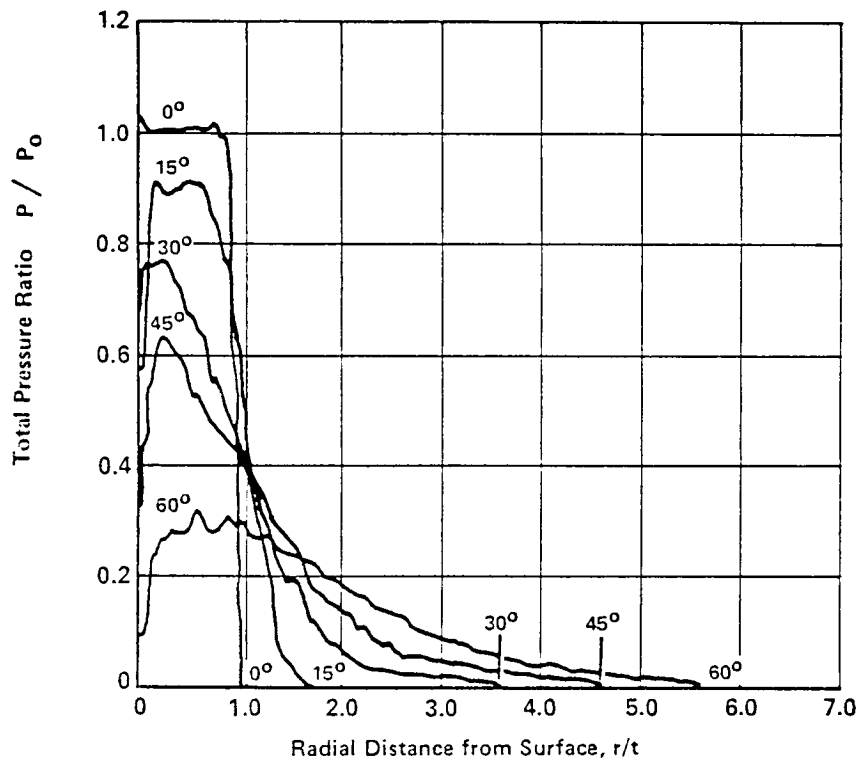


Figure 22. Symmetric Jet Total Pressure Profiles

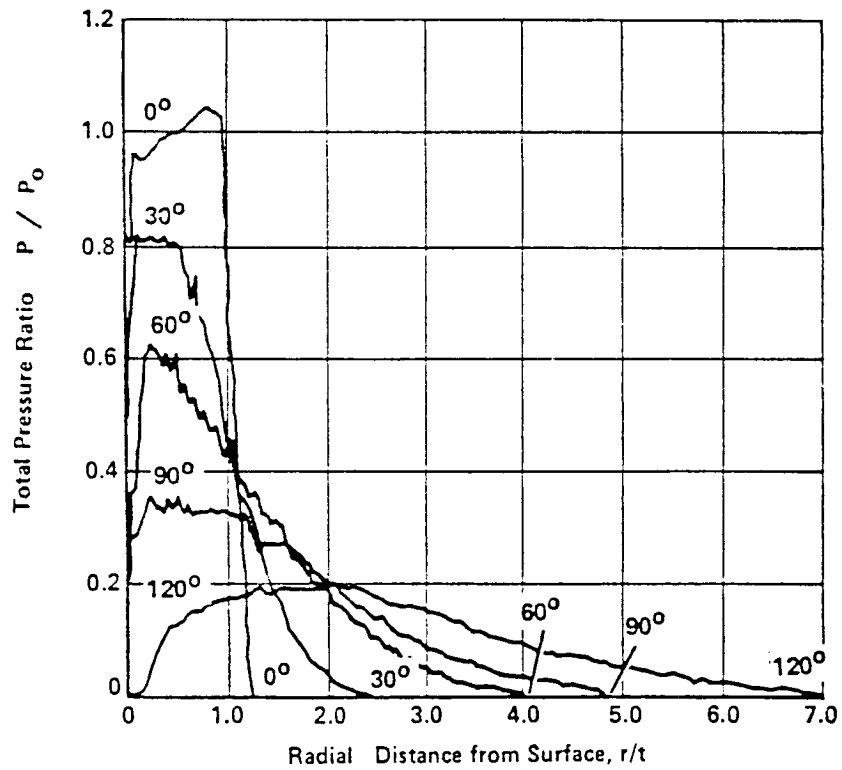


Figure 23. Vortex Jet Total Pressure Profiles

CONCLUSION

Several conclusions regarding the thrust vectoring of supersonic Coanda jets can be drawn from this study. First, the principal cause of supersonic jet detachment is boundary layer separation induced by the shocks in the wave system of the underexpanded jet. By comparing Figures 10 and 18, it can be seen that the jets from the CD nozzles detach and reattach at higher pressure ratios (3.0 and 2.2) than the jet from the convergent nozzle (2.6 and 2.0). As seen in the Schlieren photographs, the jets from the CD nozzles do detach at pressure ratios above their design point, when the shocks in the expansion wave system become strong enough to separate the boundary layer. Presumably, designing the nozzle for a higher pressure ratio would also raise the pressure ratios due to overexpansion waves. This is a subject for further investigation.

As seen in Figure 19, the thrust of the deflected jet from the vortex nozzle is approximately 5% greater than the thrust of the jet from the symmetrical CD nozzle; when the jets are detached, the thrust of the jet from the symmetrical nozzle is approximately 5% greater. Thus, there seems to be a thrust loss of this magnitude associated with adjusting the uniform profile to curvature, or the skewed profile to uniform pressure. In a deflected jet system, such as the X wing or circulation control wing, the vortex nozzle does provide more thrust. On the other hand, as seen in Figure 19, the vortex nozzle does not increase the pressure ratios for detachment or reattachment of the Coanda jet. This must be because the turning shocks in the jet with the uniform profile are not strong enough to cause detachment. At a higher pressure ratio, or for a smaller radius turn, the turning shocks in the uniform jet would be stronger and might then cause detachment. In this case, the vortex nozzle may delay detachment. However, further testing is required to determine if this is so.

To summarize, the thrust vectoring of supersonic Coanda jets may be significantly improved by the use of a convergent-divergent nozzle rather than a simple converging nozzle, because this eliminates the expansion shocks which cause boundary layer separation. On the other hand, for the pressure ratio and turning radius tested, the turning waves were not strong enough to cause detachment, so that skewing the velocity profile to match the radial pressure gradient does improve the thrust, but not the detachment pressure ratio of the deflected jet.

An improved vortex nozzle design procedure, which results in a shorter and lighter nozzle was also developed as part of this study. This procedure may also be useful for reducing the length of the vortex nozzles used to generate aerodynamic windows for gas dynamic lasers.

*ACKNOWLEDGEMENT - This study was supported in part by the Air Force Wright Aeronautical Laboratories under Contract Number F33615-79-C-3026.

REFERENCES

1. Von Glahn, U., and Groesbeck, D.: Effect of External Jet-Flow Deflector Geometry on Over-the-Wing Aero-Acoustic Characteristics. NASA TM X-73460, 1976.
2. Davenport, F. J., Hunt, D. N.: Deflection of a Thick Jet by a Convex Surface: A Practical Problem for Powered Lift. AIAA Paper 75-167, AIAA 13th Aerospace Sciences Meeting, Pasadena, California, Jan. 20-22, 1975.
3. Metral, A., Zerner, F.: The Coanda Effect. Publication Scientifiques et Techniques du Ministere de l'Air, No. 218 (1948); M.O.S., TIB/T4027 (1953).
4. Von Glahn, U.: Use of the Coanda Effect for Jet Deflection and Vertical Lift with a Multiple-Flat-Plate and Curved-Plate and Curved-Plate Deflection Surfaces. NACA TN 4377, September 1958.
5. Bradbury, L. J. S., Wood, M. N.: An Exploratory Investigation into the Deflection of Thick Jets by the Coanda Effect. Royal Aircraft Establishment, Technical Report No. 65235, October 1965.
6. Newman, B. G.: Deflection of Plane Jets by Adjacent Boundaries - Coanda Effect. Article in Boundary Layer and Flow Control, Its Principles and Application, Pergamon Press, 1961.
7. Guile, R. N., Hilding, W. E.: Investigation of a Free-Vortex Aerodynamic Window. AIAA Paper 75-122, AIAA 13th Aerospace Sciences Meeting, Pasadena, California, Jan. 20-22, 1975.
8. Liepman, H. W. and Roshko, A.: Elements of Gas Dynamics. J. Willet and Sons.
9. Dayman, B.: Comparison of Calculated with Measured Boundary Layer Thicknesses on the Curved Walls of the JPL-20-inch Supersonic Wind Tunnel Two-Dimensional Nozzle. JPL-TR No. 32-349, 1963.
10. Bevilaqua, P. M. and Lee, J. D.: Development of a Nozzle to Improve the Turning of Supersonic Coanda Jets. AFWAL TR 80-3027, April 1980.
11. Guitton, D. E., Newman, B. G.: Self-Preserving Turbulent Wall Jets over Convex Surfaces. J. Fluid Mech (1977), Vol. 81, Part I, pp. 155-185.